Arsenic and chromium partitioning in a podzolic soil contaminated by chromated copper arsenate

Luisa Hopp[1*], Peter S. Nico[2], Matthew A. Marcus[3] and Stefan Peiffer[1]

[1] Department of Hydrology, University of Bayreuth, BayCEER, 95440 Bayreuth, Germany

[2] Earth Sciences Division, Lawrence Berkeley National Laboratory, One Cyclotron Rd., Berkeley, CA 94720, USA

[3] Advanced Light Source, Lawrence Berkeley National Laboratory, One Cyclotron Rd., Berkeley CA 94720, USA

[*] Corresponding author; now at Department of Forest Engineering, Oregon State University, Corvallis, OR 97330, USA; luisa.hopp@oregonstate.edu, phone +1-541-737-8719, fax +1-541-737-4316

Abstract

This research combined the use of selective extractions and x-ray spectroscopy to examine the fate of As and Cr in a podzolic soil contaminated by chromated copper arsenate (CCA). Iron was enriched in the upper 30 cm due to a previous one-time treatment of the soil with Fe(II). High oxalate-soluble Al concentrations in the Bs horizon of the soil and micro-XRD data indicated the presence of short-range ordered aluminosilicates (i.e. proto-imogolite allophane, PIA). In the surface layers, Cr, as Cr(III), was partitioned between a mixed Fe(III)/Cr(III) solid phase that formed upon the Fe(II) application (25-50%) and a recalcitrant phase (50-75%) likely consisting of organic material such as residual CCA-treated wood. Deeper in the profile Cr appeared to be largely in the form of extractable (hydr)oxides. Throughout the soil, As was present as As(V). In the surface layers a considerable fraction of As was also associated with a recalcitrant phase, probably CCA-treated woody debris, and the remainder was associated with (hydr)oxide-like solid phases. In the Bs horizon, however, XAS and XRF findings strongly pointed to the presence of PIA acting as an effective adsorbent for As. This research shows for the first time the relevance of PIA for the adsorption of As in natural soils.

Introduction

Chromated copper arsenate (CCA) compounds have widely been used for more than six decades as very effective wood preservatives, considerably expanding the lifespan of treated wooden structures exposed to weather (*1, 2*). Arsenic and Cu act as insecticides and fungicides, respectively, while chromium is used to fix the active components to the wood matrix. The fixation process is driven by the reduction of Cr(VI) to Cr(III) by wood constituents, such as lignin and cellulose, resulting in the formation of complexes between Cr and As and lignin and between Cu^{2+} and lignin (*2-4*). However, due to the risk of arsenic toxicity, the U.S. EPA banned the use of CCA-treated wood for residential purposes at the beginning of 2004 (*5*).

Numerous studies have shown that CCA components are subject to leaching when the treated wood is exposed to environmental conditions (*6-8*). The leaching results in elevated As, Cr and Cu concentrations in the soils adjacent to the wooden structures (*9-11*). In addition, accidental spills, leakages, deposition of sludge, and dripping from freshly treated wood at wood preserving sites have led to local, often severe contamination of the soil with arsenic, chromium and copper. The risks that these sites pose for surface and subsurface waters have been recognized in the U.S. (U.S. EPA Superfund program (www.epa.gov/superfund)) and elsewhere (*12, 13*). Only a few studies have investigated the mobility and partitioning of CCA components at former wood preserving sites (*13-16*) and none have combined the analysis of the distribution of the CCA components in the soil profile with direct identification of adsorbing solid phases.

Gustafsson and Jacks (*17*) added As(V) to B horizons of podzolized forest soils and found that As(V) adsorption patterns could best be correlated with the content of ferrihydrite and proto-imogolite allophane (PIA) in the B horizons, suggesting that reactive Fe and Al phases were important adsorbents for As. Lund and Fobian (*16*) as well as Bhattacharya et al. (*14*) both demonstrated the importance of reactive Fe and Al phases in B horizon in podzolic soils for the accumulation of As and Cr. Cr was also enriched in surface layers containing organic matter.

The objective of this work was to identify soil components that are relevant for the fate of As and Cr in a podzolic soil contaminated by CCA using a combination of selective extractions and x-ray spectroscopic techniques.

Experimental section

Site description and sampling. The study was carried out on a former drip pad of a wood preserving plant in central Bavaria, Germany, where freshly impregnated wood had been stored for fixation. The site is located in the humid-temperate climatic region, with a mean annual temperature of 7.5 °C and a mean annual precipitation of 750 mm. The drip pad (69 000

m^2) was in use from 1920 until 1994. The main wood preservatives applied over this time period were chromium salts (mainly CCA) and coal tar creosotes. The detection of high chromate concentrations in the groundwater at the study site in the mid-eighties initiated a one-time application of Fe(II)-sulphate solution to the surface of the drip pad, aiming at reduction and subsequent immobilization of chromate in the soil. No records of the quantity of applied Fe(II) were available.

The soil at the experimental site developed on 20-30 m deep Pleistocene dune sand that was classified as a weathering product of Keuper sandstones (*18*). In this region the dominant soil types are Dystric Cambisols and Podzols (*19*). The depth to groundwater is approximately 4.5 m. A reference profile outside the premises was clearly classified as a Podzol. Podzolic soils are characterized by an eluvial horizon, depleted in Al and Fe, and an accumulation of Fe and Al (hydr)oxides as poorly crystalline minerals in an underlying B horizon that often has a reddish-brown coloring (*20-22*).The soil profile at the drip pad was strongly altered by the entry of creosote and exhibited a very variable profile which made the delineation of soil horizons impossible. The profile was divided into seven distinct layers (H1 – H7; Fig. 1) based mainly on visual and textural features. The upper centimeters of the profile had a dark color and contained tar crusts and tar lumps. Between 30 and 65 cm the soil exhibited a strong red brown color with crust-like, indurated structures. This layer was thought to be equivalent to a Podzol Bs horizon. Below 110 cm the transition to the original sandy material was complete. The drip pad was free of vegetation. The soil texture consisted of medium to coarse sand (fraction of silt and clay less than 1%). Bulk density increased with depth and ranged between 1.5 g cm^{-3} and 1.7 g cm^{-3}. Soil pH-values (in 0.01M $CaCl_2$) were moderately acid, ranging from pH 4.9 to pH 5.8, and showed no trend with depth.

An experimental plot with the dimensions 280 by 400 cm was divided into a grid consisting of 20 partial areas (80 x 70 cm each). A composite sample of one layer was obtained by manually sampling each of the 20 areas and thoroughly mixing the soil material in a container. After sampling of one layer the soil was manually removed and the next layer was sampled in the same manner. The profile was sampled to a depth of 200 cm. Composite samples at the reference profile were taken from the Ae (10-30 cm) and the Bs (30-40 cm) horizon. The soil samples were stored in sealed plastic containers at 4°C.

Soil characterization. Total concentrations of As, Cr, Al and Fe in layers H1-H7 were determined in hot aqua regia microwave digestion (*23*) and analyzed by inductively coupled plasma atomic emission spectroscopy (Integra XMP, GBC Scientific Equipment). The mineralogy of bulk samples from layers H2 and H4 and from the uncontaminated reference profile was determined by X-ray diffraction (XRD) with a Philips X'Pert Pro XRD system operating in reflection mode, using Co K_α radiation. The diffraction patterns were collected in the 2theta range between 7° and 90° with a 0.03° step size and a scan speed of 0.002° s^{-1}.

Selective extractions. Reactive forms of Fe and Al and associated fractions of As and Cr were characterized with selective dissolution techniques. It is generally assumed that oxalate mobilizes poorly crystalline Fe (hydr)oxides (e.g. ferrihydrite) and organic complexes of Fe (*24*) whereas a dithionite extraction additionally includes more crystalline iron phases, like goethite (*25*). For Al, oxalate extracts poorly crystalline Al hydroxide phases (including interlayer Al-hydroxy polymers), short-range ordered aluminosilicates (like imogolite and PIA), and finally organic complexes of Al (*24*). However, dithionite extracts predominantly Al^{3+} substituted for Fe^{3+} in poorly and well crystalline iron oxides (*26, 27*). Pyrophosphate is a selective extractant for organic complexes of Al and Fe, but Kaiser and Zech (*28*) showed that pyrophosphate can also extract some non-crystalline $Al(OH)_3$.

Individual one gram samples of oven-dried soil material were extracted with 100 ml of 0.2 M ammonium oxalate at pH 3 (*29*) and with 50 ml of sodium dithionite-citrate-bicarbonate (*30*), respectively. Concentrations of As, Cr, Al and Fe were determined by inductively coupled plasma atomic emission spectroscopy (Integra XMP, GBC Scientific Equipment) and will be subscripted by an o (oxalate) and d (dithionite) for the respective extractant. Dithionite-soluble Fe concentrations were also determined in the soil samples from the reference profile. For a more detailed investigation of layer H4, the layer corresponding to a Podzol Bs horizon, 1 g of air-dried soil material of this layer was extracted with 100 ml of 0.1 M pyrophosphate (*31*). Si concentrations in oxalate and Al and Si concentrations in pyrophosphate (subscript p) extracts were determined by flame atomic absorption spectroscopy (SpectrAA-20, Varian).

If possible, only polyethylene (PE) bottles and equipment were used. PE bottles for long-term storage of extracts were cleaned with 1Vol.-% nitric acid (suprapur) prior to usage. Digests and extractions were carried out in three replicates. All extracts were membrane filtered (0.45 µm cellulose acetate or nylon) prior to analysis.

X-ray spectroscopy. Arsenic and Cr bulk X-ray absorption (XAS) data on unmanipulated H2 and H4 materials were collected at the Advanced Photon Source, Argonne National Lab, Beamline 13, GeoSoilEnviroCARS. Micro x-ray fluorescence (XRF) maps of H2 and H4 were collected at Beamline 10.3.2 of the Advanced Light Source, Lawrence Berkeley National Laboratory. Micro-XRD patterns of H4 were collected using the same beamline and were converted to d-spacing using an γ-Al_2O_3 standard spectrum and the processing program FIT2D (*32*). Routine data processing (pre-edge subtraction, normalization, and extraction of the EXAFS) was done in ATHENA (*33*). Shell-by-shell EXAFS fitting was conducted using Feff7 and SixPACK (*34*). Along with the reported single scattering paths, the three multiple scattering peaks associated with the As(V) tetrahedron were included in all fits. Fits were conducted in k^3

weighted R space (1 to 6) using a k^3 weighted Kaiser-Bessel window and a k range of 4.2 to 12.5.

Results and Discussion

Total concentrations in the soil profile and mineralogy. The analysis of total elemental concentrations showed a significant enrichment of Fe, As and Cr in the top two layers of the contaminated soil (Fig. 1). Below 65 cm the concentrations decreased substantially. The Fe profile was unusual for a podzolic soil but could be explained by the application of Fe(II) that had been oxidized in the surface soil and precipitated in-situ, most likely as Fe(III) (hydr)oxides. The Al profile with its peak concentration in layer H4 reflected the podzolic nature of the soil and confirmed that this layer was equivalent to a Podzol Bs horizon.

Total concentrations of Fe and Al phases were too low and/or amorphous to be identified by XRD (detailed XRD results in Supporting Information). However, XRD data indicated the presence of the clay minerals illite and kaolinite in the layer H4 and the Bs horizon of the reference profile and showed that the contaminated profile and the reference profile were very similar with respect to their mineral composition.

Speciation of the solid phase by sequential extractions. Dithionite-extractable Fe concentrations, similar to the total Fe concentrations, decreased from top to bottom in the profile and were dramatically higher than the oxalate-soluble fraction (Fig. 1). In contrast, the dithionite-soluble Fe concentrations in the reference soil showed a typical Podzol profile of enrichment in the Bs horizon (41 ± 4 mmol kg^{-1}) compared to the Ae horizon (1.1 ± 0.2 mmol kg^{-1}). This observation strongly suggested that the unusual Fe profile at the study site was caused by the Fe(II) application which must have led to the precipitation of large quantities of Fe-containing compounds in the upper soil layers. In contrast, in the H4 layer, oxalate-extracted Fe was more than 90% of the dithionite-extractable Fe (Fig. 1) and both oxalate- and dithionite-soluble

concentrations were similar to total Fe concentrations indicating that in this layer Fe was predominantly present as poorly crystalline ferrihydrite. Therefore, layer H4 seemed to reflect the Fe geochemistry of an unaffected Podzol Bs horizon for which Fe_o:Fe_d ratios of 0.8-1 are characteristic (*25*).

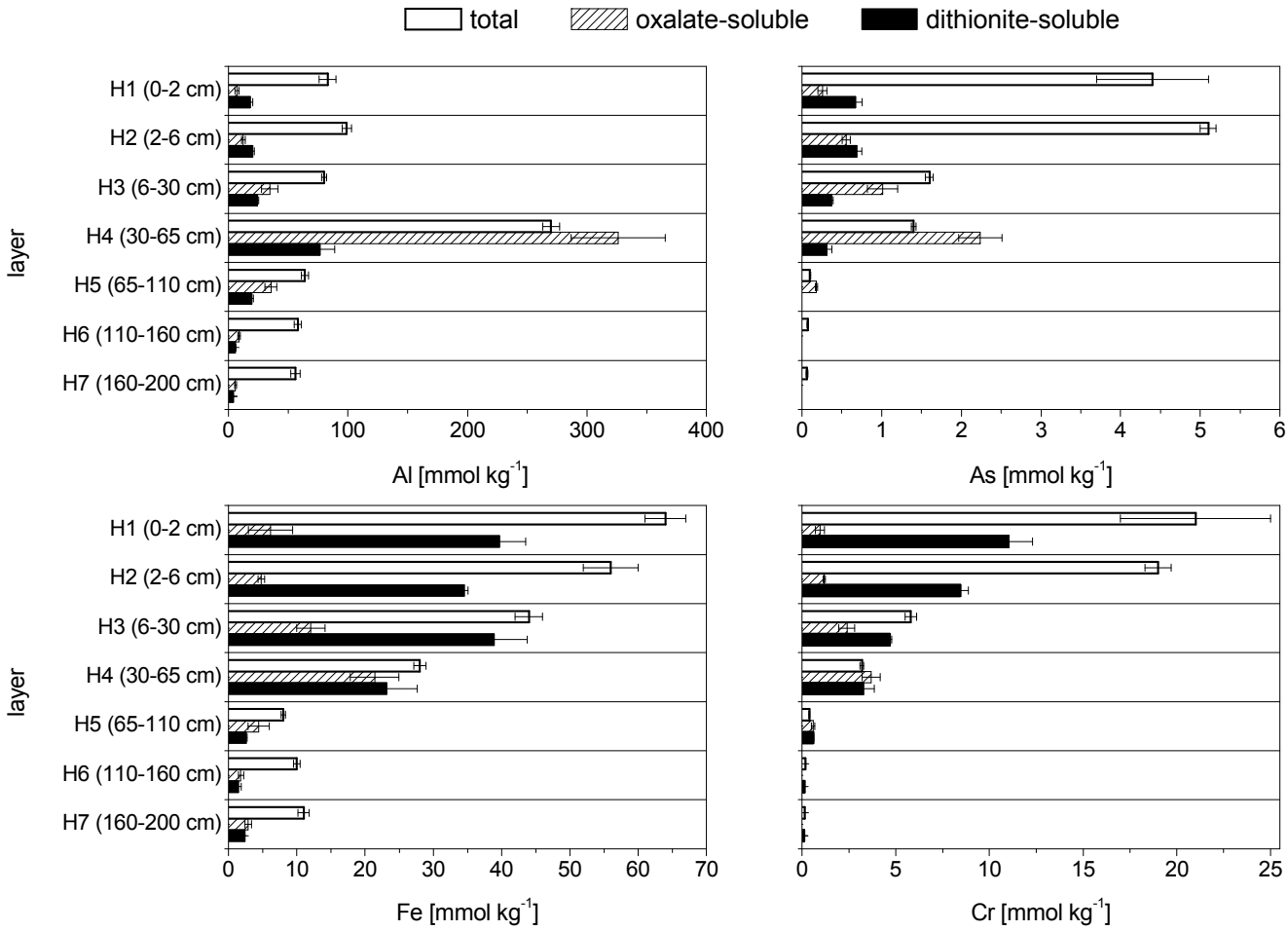

Figure 1. Concentrations of Al, Fe, As and Cr mobilized in aqua regia digests (total) and selective extractions.

Chromium showed an extraction pattern similar to Fe with dithionite extractability far exceeding that of oxalate in layers H1-H3. However, dithionite mobilized only approximately half of total Cr concentrations indicating a Cr pool present in the upper layers that was not accessible with selective extractions. Chromium entered the soil as Cr(VI) dripping off the freshly impregnated timber or as Cr(III) leached from the treated timber that was stored on the drip pad. The application of Fe(II) introduced an abundance of effective reductant for Cr(VI) (*35,*

36) probably leading to the precipitation of a poorly crystalline Cr-substituted ferrihydrite [$(Cr_xFe_{1-x})(OH)_3$] (*37, 38*). In contrast, the amount of Cr extracted by oxalate and dithionite were very similar and equaled total concentrations in layer H4 indicating that Cr is almost completely existent as a poorly crystalline phase or associated with such a phase (e.g. ferrihydrite).

Oxalate-soluble, dithionite-soluble and total Al concentrations all showed a maximum value in layer H4, with oxalate-soluble Al being roughly equal to total As concentration and dominating dithionite-soluble Al by a factor of four. The excess of oxalate-extractable Al in H4 implied the dominance of short-range ordered aluminosilicates, e.g. proto-imogolite allophane (PIA), that are known to occur in Podzol Bs horizons (*39, 40*). PIA contribute significantly to the anion adsorption capacity in Podzol B horizons due to their high point of zero charge (*41, 42*). Further evidence for the existence of PIA in layer H4 was provided by the 2.3 molar ratio of inorganic Al to inorganic Si (Supporting Information, Table SI 1), which was within the range of the expected molar ratio of soil PIA of 2-3 (*31, 43*).

Apart from layer H4, As concentrations measured in selective extractions were considerably lower than total As concentrations (Fig. 1) implying a significant pool of As not associated with metal (hydr)oxides. However, like the Fe_d/Fe_o and Cr_d/Cr_o ratio, the As_d/As_o ratio was greater than 1 in H1 and H2, suggesting that As might to some extent be associated with Fe and/or Cr in these layers. In H3 and H4, oxalate mobilized significantly higher concentrations of As than dithionite. Based on the similarity between the behavior of Al and As, we initially hypothesized that As adsorption onto PIA exerts a dominant control on As speciation in layer H4. To the best of our knowledge this would be the first report of specifically PIA-type phases controlling As speciation in a natural system.

X-ray fluorescence mapping and X-ray absorption spectroscopy of H2 and H4. Bulk Cr XANES spectra of the H2 and H4 fractions indicated that Cr was in the Cr(III) oxidation state in both layers (spectra shown in SI). Figure 2 shows the tricolor XRF map of the Cr (green), Fe (red) and As (blue) distribution in H2 and H4. The large green particles in Figure 2A indicated areas with significant concentrations of Cr and minimal concentrations of Fe or As and showed the morphology of fiber-like organic detritus. The largest of these, located in the lower center of the image, showed wood-like grain structure. The reconstruction of the bulk Cr H2 spectra using a linear combination of standards of Cr-containing phases (cf. SI) showed that only $Cr_{0.25}Fe_{0.75}(OH)_3$ and Cr in CCA-treated wood contributed significantly, 22% and 77%, respectively. These results supported the XRF observations and the results from the selective extractions, viz. a significant fraction of Cr in the upper soil layers associated with a recalcitrant phase and the existence of mixed phase $[(Cr_xFe_{1-x})(OH)_3]$ precipitates. In contrast, Figure 2B shows that in H4 while there were still some Cr-only regions (green areas), there were no large Cr-only particles like those seen in H2. The dominant yellow color in Figure 2C indicated that Fe and Cr were closely associated. While quantitative

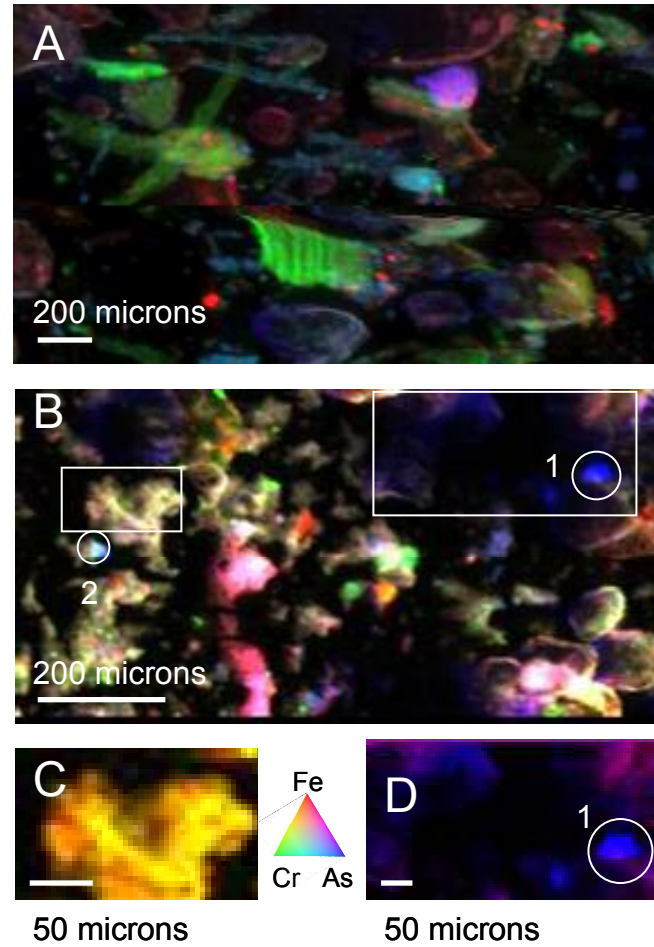

Figure 2. XRF elemental maps of Fe (red), Cr (green), and As (blue) in layers (A) H2 and (B) H4. (C) Inset from B left showing just Fe (red) and Cr (green), (D) Inset from B right showing just Fe (red) and As (blue).

interpretation of XRF images is difficult, the decrease in Cr-only particles (green areas) from H2 to H4 and the corresponding increase in regions of Cr associated with Fe again supported the results from the sequential extractions that Cr was more associated with Fe in H4 than in H2.

Figure 2A also shows that As in H2 was associated with Fe (purple areas) but also with Cr in some of the wood particles (fiber-like blue-green particles). This matched well with the sequential extraction data which indicated that in the upper layers there was an As fraction associated with Fe and a fraction not extractable with either oxalate or dithionite. In H4, there were also regions of collocated As and Fe (Fig. 2B), e.g. pinkish purple areas in the left center and lower left, but there were also significant portions of As not associated with Fe or Cr, e.g. blue regions in upper left quadrant Figure 2B and in Figure 2D. Unfortunately, due to technical limitations of the beamline used it was not possible to map Al or Si. However, it is reasonable to assume that grains that were free of significant concentrations of K, Ca, Ti, Cr, Mn, or Fe (all observable) were dominated by either Al and/or Si.

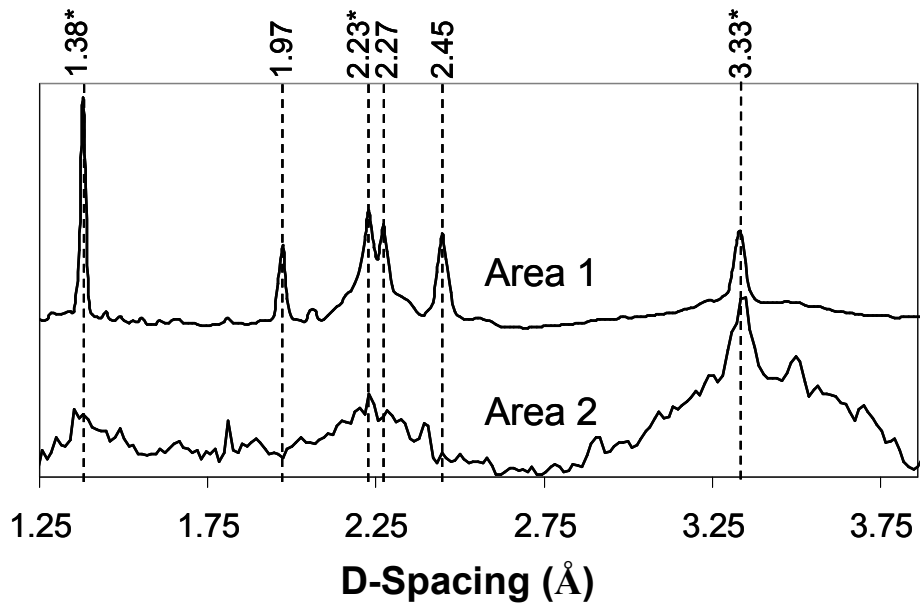

Figure 3. Micro-XRD patterns collected from layer H4 (areas 1 and 2 of Figure 2B and D). Peaks characteristic for PIA are indicated by *.

Micro-XRD data collected from layer H4 showed peaks characteristic of PIA, specifically 1.38 Å, 2.23 Å, and 3.33 Å (Fig. 3). The XRD peaks in the area 2 pattern were broad, as expected for the amorphous PIA (*21, 44*). The peaks in the area 1 pattern were sharper

indicating some degree of micro-crystallinity, but were still diagnostic for PIA, especially the 1.38 Å peak which is present in all the allophane type minerals and not in any of the other likely minerals such as Fe-oxides, gibbsite and quartz (*21, 44*). The absence of peaks at higher d-spacing, up to 16 Å, in either particle implied that these particle had minimal long range such as clay microaggregates. The three additional peaks found in the area 1 pattern were characteristic for ferrihydrite. This was likely due to presence of the overlapping Fe-containing grain that can be also be seen in area 1, Figure 2D.

Table 1. As EXAFS fitting parameters (Numbers in parenthesis are errors associated with final digit in reported value).

Sample (Model)	Shell	Coordination Number	Distance [Å]	Debye-Waller	E_0
H2 (A)	O	4*	1.680(4)	0.0011(2)	6(2)
	Fe	2*	3.23(2)	0.008(2)	6(2)
H4 (B)	O	4*	1.684(4)	0.0010(2)	8(1)
	Al	2*	3.20(1)	0.001(1)	8(1)
H4 (C)	O	4	1.683(4)	0.0010(2)	8(1)
	Al	1.5(3)	3.23(3)	0.001*	8(1)
	Fe	0.5	3.27(2)	0.001*	8(1)

*Fixed Parameter; S_0^2 fixed at 0.9

Vertically expanded views of the H2 and H4 As XANES spectra are shown in Figure 4 (full spectra along with a Na_3AsO_4 standard in SI). The edge position of both spectra was indicative of As(V) which was consistent with results showing that As is predominantly leached from CCA as As(V) (*6, 45*). Differences in the spectra revealed that the average speciation of As changed from H2 to H4. The H4 spectra was similar to those published by Arai et al. (*46*) of As(V) sorbed on γ-

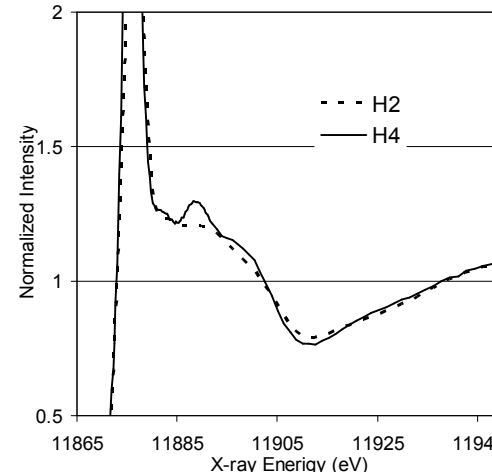

Figure 4. As XANES spectra of H2 and H4, vertically expanded.

Al_2O_3, supporting the hypothesis that As was associated with Al in this layer. Figure 5A, B and C show the Fourier transform EXAFS data from the H2 and H4 and the corresponding fits from Table 1. The best model fit for layer H2 was obtained using the A model which is a bidentate binuclear complex between As(V) tetrahedron and two Fe octahedral with the distances shown in Table 1. The As-O and As-Fe distances in Table 1 matched very well with those previously reported for As bound to Fe (hydr)oxides (*47*). They were also very similar to the distance expected from an As-Cr backscattering pair present in As bound in CCA-treated wood (*4*). Substitution of Cr for Fe in the H2 fits produced similar fits, allowing the possibility of As bound to either Fe or Cr. Therefore, the EXAFS data supported the hypothesis that extractable As in the H2 fraction was most likely bound to Fe while also allowing that the non-extractable fraction of As could be that associated with CCA-treated wood debris.

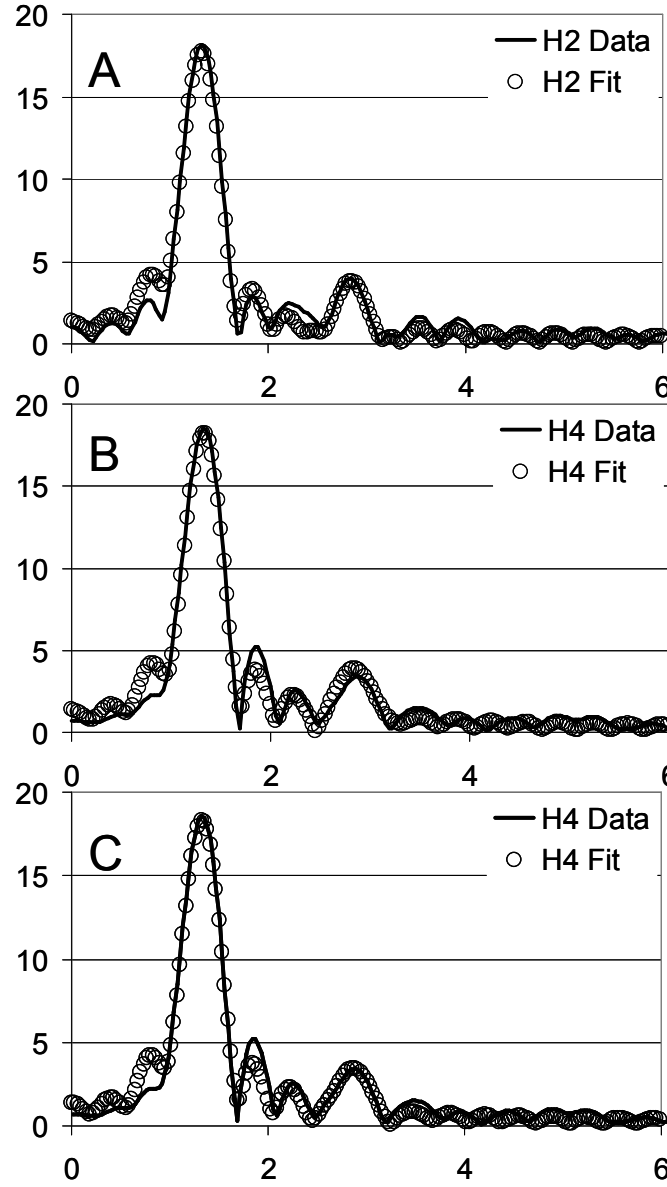

Figure 5. Fourier transform EXAFS data from layers H2 (A) and H4 (B, C) and corresponding fits from Table 1.

In contrast, the H4 spectrum was fit well by model B which is a bidentate binuclear complex between an As tetrahedron and two Al octahedral, Figure 5B and Table 1. This Al shell

appeared at ~3.2 Å which fits within the range of As(V)-Al bond distances previously reported: 3.1 Å on γ-Al_2O_3 as bidentate-binuclear complex (*46*), 2.6 Å on γ-Al_2O_3 as a binuclear-monodentate complex (*48*) 3.19 Å on allophane (*44*), and 2.54 Å in natural soil samples (*49*). While the extraction data, the micro-XRD and the EXAFS fitting all pointed to the binding of As to PIA in H4, the binding of As to Fe(hydr)oxides cannot be ruled out by the EXAFS fits. As seen in Figure 5C, the fit to H4 is slightly improved by including both binding modes, i.e. model A and B. The relative contribution of the two binding modes were estimated based on the coordination numbers in Table 1 and were ~75% As bound to Al and ~25% As bound to Fe. These data strongly supported the hypothesis that As was primarily associated with PIA type minerals in the H4 layer, while accounting for the Fe-associated As observed in Figure 2D.

Conceptual model for the behavior of As and Cr in the sampled soil. The selective extractions indicated that the major sorption capacity of the soil is located within the upper 65 cm (layers H1 to H4). The application of Fe(II) and subsequent formation of mixed Fe(III)-Cr(III) minerals immobilized chromate and at the same time increased the content of soil adsorbents in the upper soil layers. However, a large fraction of the Cr in H2 appears to be bound to organic phases, e.g. CCA-treated wood debris. This pool of Cr appears to be the most stable phase. Cr that was not retained in upper soil layers was adsorbed to amorphous Fe minerals in the layer that corresponded to a podzolic Bs horizon (H4).

Arsenic entered the soil either by dripping of surplus CCA solution, leaching from the treated timber during storage or associated with CCA-treated wood debris. Arsenic in the CCA formulation is in the As(V) state and the As XAS data confirmed that As has maintained its oxidized state. Free arsenate reaching the soil was either adsorbed to Fe and/or Fe-Cr phases or was leached into deeper layers. The difference between extractable and total As concentrations and the observation of organic particles with significant As and Cr concentrations in the XRF

mapping imply that a large fraction of As is associated with CCA-treated wood or other organic debris. This wood-associated pool constitutes a significant and still active source of As that will likely continue to leach slowly for an extended period of time. Deeper in the soil profile, the podzolic B horizon with its high concentration of Al in the form of high sorption capacity PIA is concentrating downward moving arsenate. Below this horizon (> 65 cm) the sorption capacity of the soil decreases considerably. Therefore, As and Cr that are leached beyond this depth will most likely be transported into the groundwater. The sampling of groundwater (depth approximately 4.5 m below the ground surface) over a period of 10 weeks in 2004 (*50*) showed elevated Cr concentrations (50-330 ppb) but only low concentrations of As (< 12 ppb), suggesting that for the time being the podzolic B horizon is providing an effective barrier for As. This research contributes to the understanding of the environmental fate of CCA-derived As and Cr in soils and strongly suggests that PIA materials are relevant for the adsorption of anions such as arsenate in natural soils.

Acknowledgements

This research was funded by the Bavarian State Department of Environment (contract no. 55-8740.1-2000/BT). The ALS and APS are supported by the Director, Office of Science, Office of Basic Energy Science, of the U.S. Department of Energy under contract no. DE-AC02-05CH11231 and DE-AC02-06CH11357, respectively. GeoSoilEnviroCARS is supported by the National Science Foundation-Earth Science (EAR-0622171), Department of Energy-Geosciences (DE-FG02-94ER14466) and the State of Illinois. Partial support was provided by U.S. Department of Energy, Office of Biological and Environmental Research, Environmental Remediation Sciences Program under contract no. DE-AC02-05CH11231. The authors are grateful to Dr. Tiziana Boffa-Ballaran, Bavarian Research Institute of Experimental

Geochemistry and Geophysics (Bayerisches Geoinstitut), University of Bayreuth, Germany, for conducting bulk XRD measurements.

Supporting Information Available

Results of XRD measurements. Additional extraction results. Additional XANES spectra for As and Cr. This information is available free of charge via the Internet at http://pubs.acs.org.

References

(1) Humphrey, D. G. The chemistry of chromated copper arsenate wood preservatives. *Rev. Inorg. Chem.* **2002,** *22*, 1-40.

(2) Hingston, J. A.; Collins, C. D.; Murphy, R. J.; Lester, J. N. Leaching of chromated copper arsenate wood preservatives: a review. *Environ. Pollut.* **2001,** *111*, 53-66.

(3) Bull, D. C.; Harland, P. W.; Vallance, C.; Foran, G. J. EXAFS study of chromated copper arsenate timber preservative in wood. *J. Wood Sci.* **2000,** *46*, 248-252.

(4) Nico, P. S.; Fendorf, S. E.; Lowney, Y. W.; Holm, S. E.; Ruby, M. V. Chemical structure of arsenic and chromium in CCA-treated wood: Implications of environmental weathering. *Environ. Sci. Technol.* **2004,** *38*, 5253-5260.

(5) U.S.-EPA. Chromated Copper Arsenate (CCA). http://www.epa.gov/oppad001/reregistration/cca/ (May 25, 2008).

(6) Khan, B. I.; Solo-Gabriele, H. M.; Townsend, T. G.; Cai, Y. Release of arsenic to the environment from CCA-treated wood. 1. Leaching and speciation during service. *Environ. Sci. Technol.* **2006,** *40*, 988-993.

(7) Lebow, S.; Williams, R. S.; Lebow, P. Effect of simulated rainfall and weathering on release of preservative elements from CCA treated wood. *Environ. Sci. Technol.* **2003,** *37*, 4077-4082.

(8) Taylor, J. L.; Cooper, P. A. Leaching of CCA from lumber exposed to natural rain aboveground. *Forest Prod. J.* **2003,** *53*, 81-86.

(9) Zagury, G. J.; Samson, R.; Deschenes, L. Occurrence of metals in soil and ground water near chromated copper arsenate-treated utility poles. *J. Environ. Qual.* **2003,** *32*, 507-514.

(10) Chirenje, T.; Ma, L. Q.; Clark, C.; Reeves, M. Cu, Cr and As distribution in soils adjacent to pressure-treated decks, fences and poles. Environ. Pollut. 2003, 124, 407-417.

(11) Stilwell, D. E.; Graetz, T. J. Copper, chromium, and arsenic levels in soil near highway traffic sound barriers built using CCA pressure-treated wood. *Bull. Environ. Contam. Toxicol.* **2001,** *67*, 303-308.

(12) Lindberg, J.; Sterneland, J.; Johansson, P. O.; Gustafsson, J. P. Spodic material for in situ treatment of arsenic in ground water. *Ground Water Monit. R.* **1997,** *17*, 125-130.

(13) Andersen, S.; Rasmussen, G.; Snilsberg, P.; Amundsen, C. E.; Westby, T. Assessing toxicity and mobilisation of impregnation salts at a contaminated site. *Fresen. J. Anal. Chem.* **1996,** *354*, 676-680.

(14) Bhattacharya, P.; Mukherjee, A. B.; Jacks, G.; Nordqvist, S. Metal contamination at a wood preservation site: characterisation and experimental studies on remediation. *Sci. Total Environ.* **2002,** *290*, 165-180.

(15) Jang, Y. C.; Townsend, T. G.; Ward, M.; Bitton, G. Leaching of arsenic, chromium, and copper in a contaminated soil at a wood preserving site. *Bull. Environ. Contam. Toxicol.* **2002,** *69*, 808-816.

(16) Lund, U.; Fobian, A. Pollution of two soils by arsenic, chromium and copper, Denmark. *Geoderma*

1991, *49*, 83-103.

(17) Gustafsson, J. P.; Jacks, G. Arsenic Geochemistry in Forested Soil Profiles as Revealed by Solid-Phase Studies. *Appl. Geochem.* **1995,** *10*, 307-315.

(18) Habbe, K. A. Die äolischen Sandablagerungen vor dem Stufenhang der Nördlichen Frankenalb - Probleme, Beobachtungen, Schlussfolgerungen. *Mitteilungen der Fränkischen Geographischen Gesellschaft* **1997,** *44*, 1-73.

(19) Schilling, B.; Hammerl, J. *Die Böden Bayerns - Handbuch für die Böden des Keuper-Lias-Landes in Franken*; Bayerisches Geologisches Landesamt: München, 2002.

(20) Melkerud, P.-A.; Bain, D. C.; Jongmans, A. G.; Tarvainen, T. Chemical, mineralogical and morphological characterization of three podzols developed on glacial deposits in Northern Europe. *Geoderma* **2000,** *94*, 125-148.

(21) Sumner, M. E. *Handbook of Soil Science*; CRC Press LLC: Boca Raton, 1999.

(22) USDA-NRCS. *Soil Taxonomy, A Basic System of Soil Classification for Making and Interpreting Soil Surveys*; United States Department of Agriculture, Natural Resources Conservation Service: Washington, DC, 1999. Available at http://soils.usda.gov/.

(23) DIN-EN-13346. Characterization of sludges - Determination of trace elements and phosphorus - Aqua regia extraction methods. *Beuth Verlag, Berlin* **2001**.

(24) Farmer, V. C.; Russell, J. D.; Smith, B. F. L. Extraction of Inorganic Forms of Translocated Al, Fe and Si from a Podzol Bs Horizon. *J. Soil Sci.* **1983,** *34*, 571-576.

(25) Cornell, R. M.; Schwertmann, U. *The Iron Oxides*; Wiley-VCH Verlag GmbH & Co. KGaA: Weinheim, 2003.

(26) Agbenin, J. O. Extractable iron and aluminum effects on phosphate sorption in a savanna alfisol. *Soil Sci. Soc. Am. J.* **2003,** *67*, 589-595.

(27) Dahlgren, R. A.; Ugolini, F. C. Distribution and Characterization of Short-Range-Order Minerals in Spodosols from the Washington Cascades. *Geoderma* **1991,** *48*, 391-413.

(28) Kaiser, K.; Zech, W. Defects in estimation of aluminum in humus complexes of podzolic soils by pyrophosphate extraction. *Soil Sci.* **1996,** *161*, 452-458.

(29) Schwertmann, U. Differenzierung der Eisenoxide des Bodens durch Extraktion mit Ammoniumoxalat-Loesung. *Zeitschrift fuer Pflanzenernaehrung, Duengung und Bodenkunde* **1964,** *105*, 194-202.

(30) Mehra, O. P.; Jackson, M. L. Iron Oxide Removal from Soils and Clays by Dithionite-Citrate System buffered with Sodium Bicarbonate. *Clays Clay Miner.* **1960,** *7*, 317-327.

(31) Karltun, E.; Bain, D. C.; Gustafsson, J. P.; Mannerkoski, H.; Murad, E.; Wagner, U.; Fraser, A. R.; McHardy, W. J.; Starr, M. Surface reactivity of poorly-ordered minerals in podzol B horizons. *Geoderma* **2000,** *94*, 265-288.

(32) Hammersley, A. P. *FIT2D: An Introduction and Overview*. European Synchrotron Radiation Facility, Internal Report ESRF97HA02T, **1997**.

(33) Ravel, B.; Newville, M. ATHENA, ARTEMIS, HEPHAESTUS: data analysis for X-ray absorption spectroscopy using IFEFFIT. *J. Synchrotron Radiat.* **2005,** *12*, 537-541.

(34) Webb, S. SixPACK, Sam's Interface for XAS Package, version 0.52. http://www-ssrl.slac.stanford.edu/~swebb/sixpack.htm (February 26, 2008).

(35) Saleh, F. Y.; Parkerton, T. F.; Lewis, R. V.; Huang, J. H.; Dickson, K. L. Kinetics of chromium transformations in the environment. *Sci. Total Environ.* **1989,** *86*, 25-41.

(36) Eary, L. E.; Rai, D. Chromate Removal from Aqueous Wastes by Reduction with Ferrous Ion. *Environ. Sci. Technol.* **1988,** *22*, 972-977.

(37) Loyaux-Lawniczak, S.; Refait, P.; Ehrhardt, J. J.; Lecomte, P.; Genin, J. M. R. Trapping of Cr by formation of ferrihydrite during the reduction of chromate ions by Fe(II)-Fe(III) hydroxysalt green rusts. *Environ. Sci. Technol.* **2000,** *34*, 438-443.

(38) Buerge, I. J.; Hug, S. J. Kinetics and pH dependence of chromium(VI) reduction by iron(II). *Environ. Sci. Technol.* **1997,** *31*, 1426-1432.

(39) Childs, C. W.; Parfitt, R. L.; Lee, R. Movement of Aluminum as an Inorganic Complex in Some Podzolized Soils, New-Zealand. *Geoderma* **1983,** *29*, 139-155.

(40) Gustafsson, J. P.; Bhattacharya, P.; Karltun, E. Mineralogy of poorly crystalline aluminium phases in the B horizon of Podzols in southern Sweden. *Appl. Geochem.* **1999,** *14*, 707-718.

(41) Clark, C. J.; McBride, M. B. Cation and Anion Retention by Natural and Synthetic Allophane and Imogolite. *Clays Clay Miner.* **1984,** *32*, 291-299.

(42) Gustafsson, J. P.; Bhattacharya, P.; Bain, D. C.; Fraser, A. R.; McHardy, W. J. Podzolisation Mechanisms and the Synthesis of Imogolite in Northern Scandinavia. *Geoderma* **1995,** *66*, 167-184.

(43) Simonsson, M.; Berggren, D. Aluminium solubility related to secondary solid phases in upper B horizons with spodic characteristics. *Eur. J. Soil Sci.* **1998,** *49*, 317-326.

(44) Arai, Y.; Sparks, D. L.; Davis, J. A. Arsenate adsorption mechanisms at the allophane - water interface. *Environ. Sci. Technol.* **2005,** *39*, 2537-2544.

(45) Khan, B. I.; Solo-Gabriele, H. M.; Dubey, B. K.; Townsend, T. G.; Cai, Y. Arsenic speciation of solvent-extracted leachate from new and weathered CCA-treated wood. *Environ. Sci. Technol.* **2004,** *38*, 4527-4534.

(46) Arai, Y.; Elzinga, E. J.; Sparks, D. L. X-ray absorption spectroscopic investigation of arsenite and arsenate adsorption at the aluminum oxide-water interface. *J. Colloid Interf. Sci* **2001,** *235*, 80-88.

(47) Waychunas, G. A.; Rea, B. A.; Fuller, C. C.; Davis, J. A. Surface-Chemistry of Ferrihydrite .1. Exafs Studies of the Geometry of Coprecipitated and Adsorbed Arsenate. *Geochim. Cosmochim. Acta* **1993,** *57*, 2251-2269.

(48) Arai, Y.; Sparks, D. L. Residence time effects on arsenate surface speciation at the aluminum oxide-water interface. *Soil Sci.* **2002,** *167*, 303-314.

(49) Arcon, L.; van Elteren, J. T.; Glass, H. J.; Kodre, A.; Slejkovec, Z. EXAFS and XANES study of arsenic in contaminated soil. *X-Ray Spectrom.* **2005,** *34*, 435-438.

(50) Hopp, L.; Peiffer, S.; Durner, W. Spatial variability of arsenic and chromium in the soil water at a former wood preserving site. *J. Contam. Hydrol.* **2006,** *85*, 159-178.

Table of Contents/Brief

This study combines selective extractions and x-ray spectroscopy to illuminate the fate of As and Cr in a soil contaminated by the wood preservative CCA.